Expanded View Figures

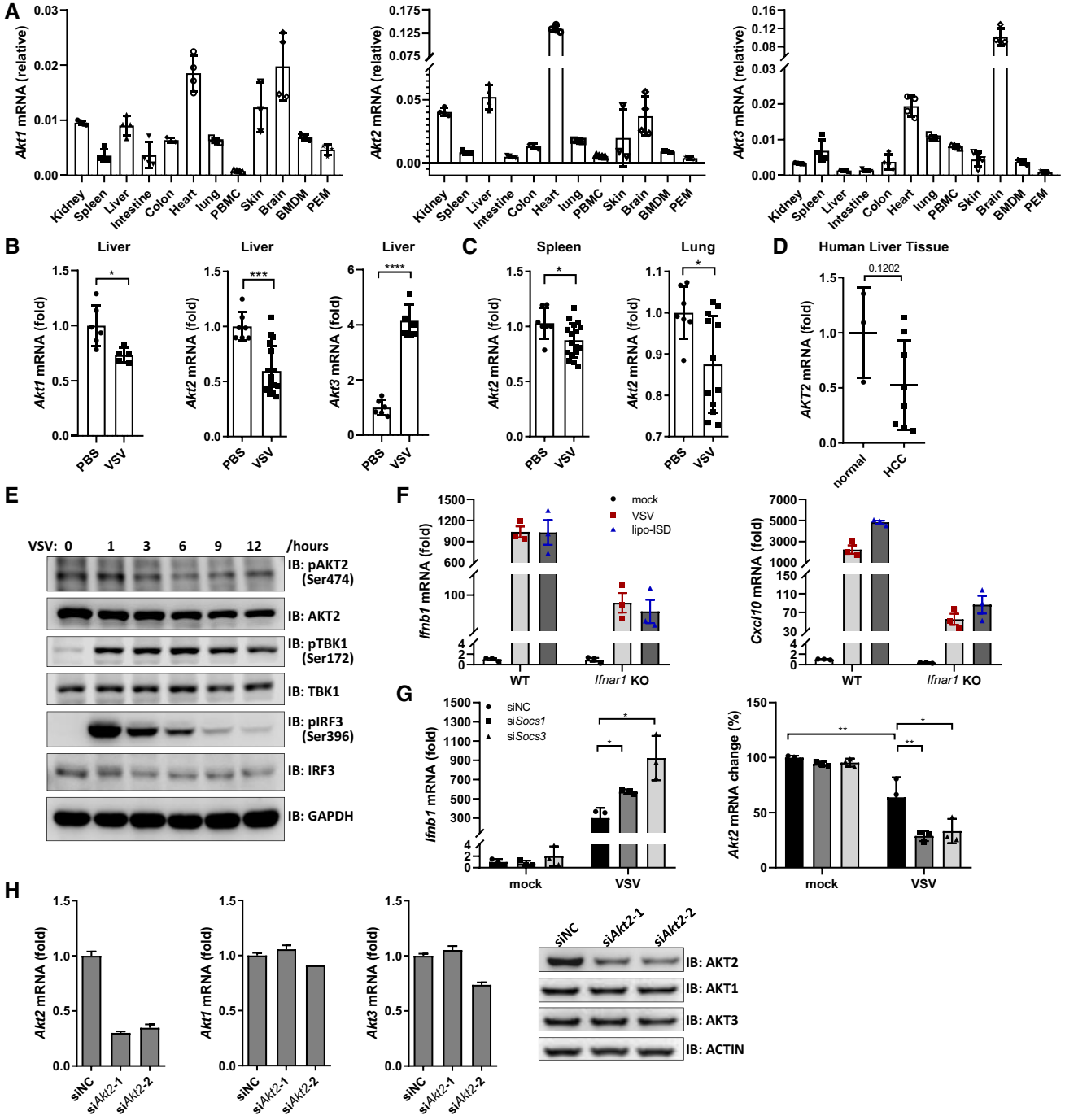

Figure EV1.

Figure EV1. The reduced *Akt2* expression and the verification of *Akt2* siRNAs efficacy (related to Fig 1).

A qRT–PCR analysis for the mRNA expression of *Akt1* ($n \geq 3$), *Akt2* ($n \geq 3$), *Akt3* ($n = 4$) in the different tissues of at least three different WT C57BL/6 mice.

B, C The mRNA expression of *Akt1*, *Akt2*, or *Akt3* in the liver, spleen, or lung from WT mice after the VSV infection for 6 h (1×10^6 PFU/g, i.v.) were detected by qRT–PCR. *Akt1* in liver, $n \geq 5$; *Akt2* in liver, $n \geq 7$; *Akt3* in liver, $n \geq 5$; *Akt2* in spleen, $n \geq 7$; *Akt2* in lung, $n \geq 7$.

D qRT–PCR analysis for the mRNA expression of *AKT2* in the liver tissue of the normal individuals ($n = 3$) or HBV-infected different HCC patients ($n = 8$).

E Immunoblot analysis of p-AKT2 (Ser473), AKT2, p-TBK1 (Ser172), TBK1, p-IRF3 (Ser396), IRF3 and GAPDH in the VSV-stimulated PEMs at indicated time points.

F The mRNA expression of *Ifnb1* and *Cxcl10* were measured by qRT–PCR in the WT and *Ifnar1* KO PEMs stimulated with VSV and lipo-ISD for 6 h. $n = 3$, respectively.

G qRT–PCR analysis for the mRNA expression of *Ifnb1* ($n = 3$, left panel) and then, the mRNA change of *Akt2* ($n = 3$, right panel) were further calculated by compared with "siNC mock" in the PEMs with *Socs1* or *Socs3* knockdown followed by stimulation of VSV for 6 h.

H The mRNA level (left panel, by qRT–PCR) and protein expression (right panel, by immunoblot) of AKT2, AKT1, AKT3 in WT PEMs transfected with siNC, si*Akt2*-1, or si*Akt2*-2 for 48 h.

Data information: $*P < 0.05$, $**P < 0.01$, $***P < 0.001$, and $****P < 0.0001$; using unpaired *t*-test (B–D), or two-way ANOVA test (G). Data are pooled from at least three independent experiments (B, C, F, G) or representative of three independent biological replicates (A, E, H). Error bars (A-D, H, mean ± SD; F and G, mean ± SEM).
Source data are available online for this figure.

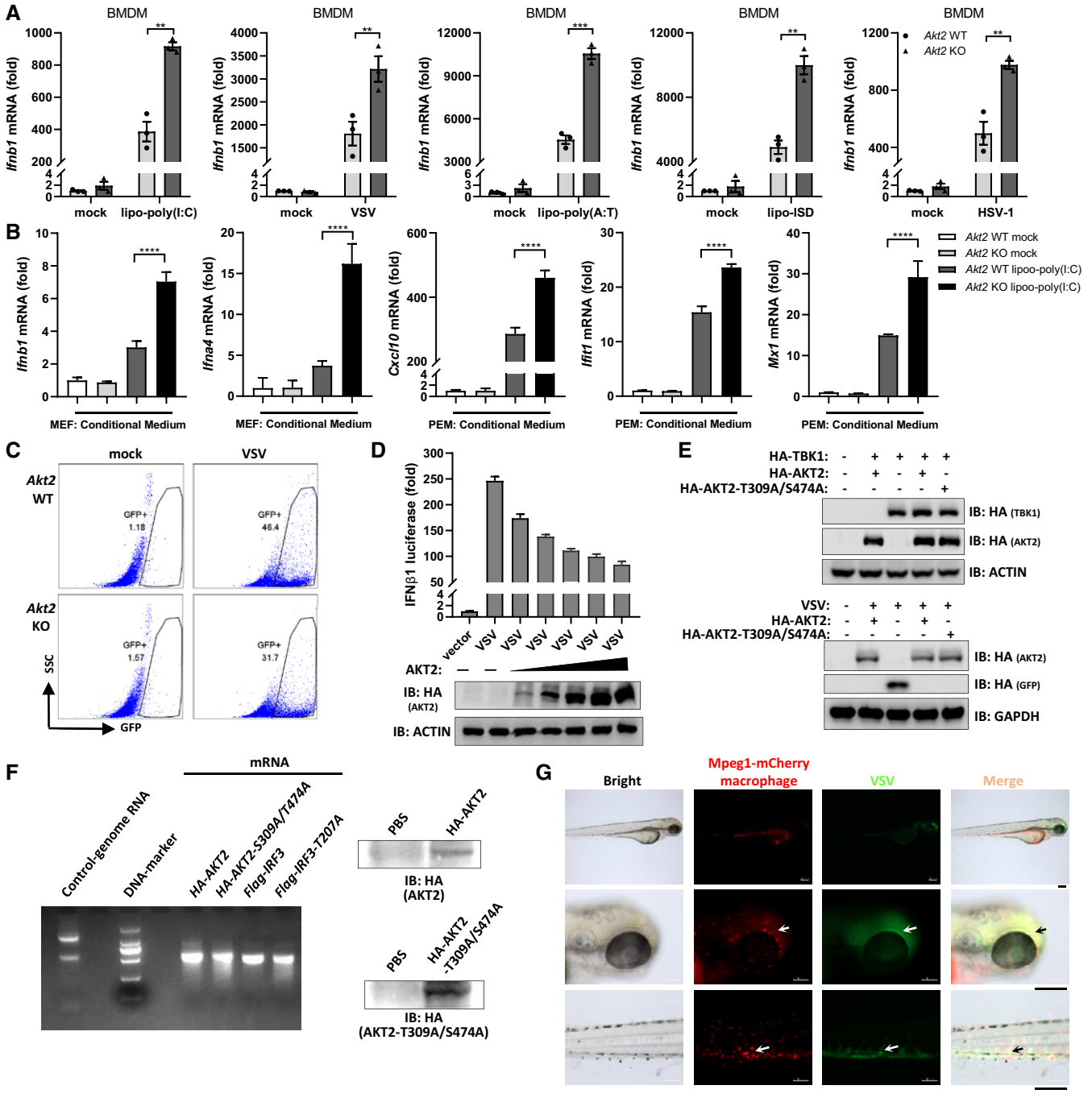
A
BMDM
Ifnb1 mRNA (fold)
mock
lipo-poly(I:C)
VSV
lipo-poly(A:T)
lipo-ISD
HSV-1
Akt2 WT
Akt2 KO
B
Ifnb1 mRNA (fold)
Ifna4 mRNA (fold)
Cxcl10 mRNA (fold)
Ifit1 mRNA (fold)
Mx1 mRNA (fold)
MEF: Conditional Medium
PEM: Conditional Medium
Akt2 WT mock
Akt2 KO mock
Akt2 WT lipoo-poly(I:C)
Akt2 KO lipoo-poly(I:C)
C
mock
VSV
Akt2 WT
Akt2 KO
GFP+ 1.18
GFP+ 46.4
GFP+ 1.57
GFP+ 31.7
SSC
GFP
D
IFNβ1 luciferase (fold)
vector
VSV
AKT2:
IB: HA (AKT2)
IB: ACTIN
E
HA-TBK1:
HA-AKT2:
HA-AKT2-T309A/S474A:
IB: HA (TBK1)
IB: HA (AKT2)
IB: ACTIN
VSV:
IB: HA (GFP)
IB: GAPDH
F
mRNA
Control-genome RNA
DNA-marker
HA-AKT2
HA-AKT2-S309A/T474A
Flag-IRF3
Flag-IRF3-T207A
PBS
IB: HA (AKT2)
IB: HA (AKT2-T309A/S474A)
G
Bright
Mpeg1-mCherry macrophage
VSV
Merge

Figure EV2.

Figure EV2. Akt2 absence facilitates the cellular antiviral responses and zebrafish larva is a suitable model for protein overexpression or VSV infection (related to Fig 2).

A Determination of the *Ifnb1* mRNA expression by qRT–PCR in M-CSF (20 ng/ml) induced BMDMs stimulated with lipo-poly(I:C), VSV, lipo-poly(A:T), lipo-ISD or HSV-1 for 6 h. $n = 3$, respectively.
B The mRNA expression levels of indicated genes were analyzed by qRT–PCR in MEFs (*Ifnb1* and *Ifna4*) and PEMs (*Cxcl10, Ifit1 and Mx1*) which were treated with conditional medium for 3 h.
C FACS analysis of the viral load indicated by GFP in primary WT and *Akt2* KO MEFs.
D IFNβ1 luciferase activity was measured in HEK293T cells transfected with empty vector or AKT2 at increasing amount for 24 h and infected by VSV for another 6 h, respectively. Immunoblot analysis showed the indicated constructs in HEK293T cells.
E The protein levels of indicated constructs as showed in Fig 2F were measured by immunoblot analysis.
F The *in vitro* transcriptional mRNAs were verified by agarose gel electrophoresis (left panel) and its translation in zebrafish larvae for 48 h were verified by immunoblot analysis (right panel).
G Representative images of mpeg1-mCherry macrophages (Red) and VSV-infected area (GFP) were collected by fluorescence microscopy in the brain and abdominal vessel (arrows) of zebrafish larvae as showed in Fig 2G. Bars, 200 μm.

Data information: $^{**}P < 0.01$, $^{***}P < 0.0011$, $^{****}P < 0.0001$; using a one-way ANOVA test (B) or two-way ANOVA test (A). Data are from three independent experiments (A) or representative of three independent biological replicates (B–G). Error bars (A, mean ± SEM; B and D, mean ± SD).
Source data are available online for this figure.

Figure EV3. AKT2 interacts with 14-3-3ε and IRF3 to slack IFNβ1 production (related to Fig 3).

A IFNβ1 luciferase activity was measured (top panel, $n = 3$) in HEK293T cells transfected with indicated constructs. Immunoblot analysis showed the indicated constructs in HEK293T cells (bottom panels).
B Immunoblot analysis of *IRF3* in HEK293T and HEK293T-*IRF3* KO cells.
C qRT–PCR analysis for knockdown efficiency of *Irf3* siRNAs (si*Irf3*-1 and si*Irf3*-2).
D WT and *Akt2* KO PEMs were treated with or without VSV or HSV-1 for 6 h, and then, the *Irf3* mRNA level was measured by qRT–PCR. $n = 3$, respectively.
E Schematic diagram of constructs expressing HA-tagged human AKT2, Flag-tagged human IRF3 and their mutants (left panel). HEK293T cells were co-transfected with indicated constructs for 24 h. Anti-HA and anti-Flag antibody-conjugated agarose beads were used for immunoprecipitation, and the interaction domain was mapped by immunoblot analysis with the indicated antibodies (right panel).
F Immunoassay of IRF3 in dimer or monomer form by native-gel and p-IRF3 (Ser396), p-TBK1 (Ser172), AKT2 and GAPDH by SDS-gel in WT and *Akt2* KO PEMs with lipo-ISD stimulation for 6 h.
G Immunofluorescent microscopic imaging (left panel) and statistics analysis (right panel, $n = 3$) for IRF3 nuclear translocation in lipo-ISD stimulated WT and *Akt2* KO PEMs. IRF3 (red), Nuclei (Hoechst, green). The white arrows indicate the nuclei with IRF3 translocation. Bar, 10 μm.
H Immunoprecipitation with anti-Myc antibody-conjugated agarose beads and immunoblot analysis about the interactions between HA-AKT2 and Myc-14-3-3ζ or Myc-14-3-3ε in HEK293T cells after overexpression of indicated constructs for 24 h.
I The mRNA level of 14-3-3ζ ($n = 4$) was measured by qRT–PCR in WT PEMs transfected the two *14-3-3ζ* siRNAs (si*14-3-3ζ*-1 and si*14-3-3ζ*-2) for 48 h (left panel). The mRNA level of *Ifnb1* ($n = 3$) was determined by qRT–PCR in VSV-stimulated PEMs that were transfected with si*14-3-3ζ*-1 (middle panel). IFNβ1 luciferase activity ($n = 3$) was measured in HEK293T cells after being transfected with empty vector or 14-3-3ζ for 24 h and treated with VSV for 6 h, and immunoblot analysis showed the indicated constructs (right panel).
J The functional verifications of *14-3-3ε* (left and right panels) as those of *14-3-3ζ* in Fig EV3I (left and middle panels, respectively).
K HEK293T cells were transfected with Flag-IRF3, HA-AKT2, and Myc-14-3-3ε. 24 h post-transfection, cells were collected and subjected to immunoprecipitation (anti-Flag antibody-conjugated agarose beads) and immunoblot.
L Immunoassay of the p-IRF3 (Ser396) and dimerization of IRF3 in HEK293T cells with the overexpression of the indicated plasmids.

Data information: $^{*}P < 0.05$, $^{**}P < 0.01$ and ns, not significant ($P > 0.05$); using a one-way ANOVA test (A left panel, I right panel) or two-way ANOVA test (D, G right panel, I middle panel and J right panel). Data are from at least three independent experiments (A left panel, D, G right panel, I and J) or representative of three independent biological replicates (A right panel, B, C, E right panel, F, G left panel, H, K and L). Error bars (A left panel, D, G right panel, I and J, mean ± SEM; A right panel and C, mean ± SD).
Source data are available online for this figure.

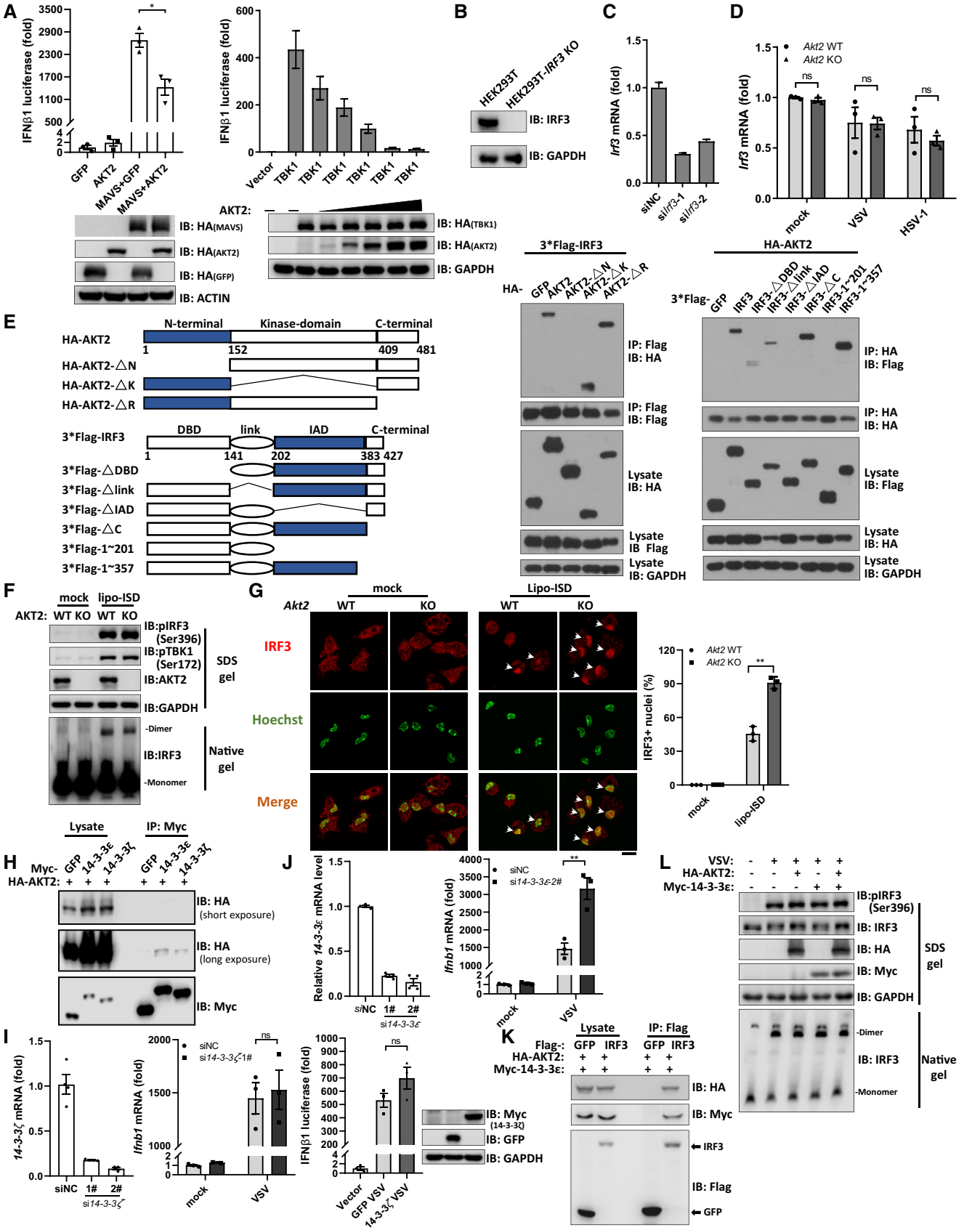
A
IFNβ1 luciferase (fold)
GFP
AKT2
MAVS+GFP
MAVS+AKT2
IB: HA(MAVS)
IB: HA(AKT2)
IB: HA(GFP)
IB: ACTIN
Vector
TBK1
AKT2:
IB: HA(TBK1)
IB: HA(AKT2)
IB: GAPDH
B
HEK293T
HEK293T-IRF3 KO
IB: IRF3
IB: GAPDH
C
Irf3 mRNA (fold)
siNC
siIrf3-1
siIrf3-2
D
Akt2 WT
Akt2 KO
ns
mock
VSV
HSV-1
E
HA-AKT2
N-terminal
Kinase-domain
C-terminal
HA-AKT2-△N
HA-AKT2-△K
HA-AKT2-△R
3*Flag-IRF3
DBD
link
IAD
3*Flag-△DBD
3*Flag-△link
3*Flag-△IAD
3*Flag-△C
3*Flag-1~201
3*Flag-1~357
3*Flag-IRF3
HA-AKT2
IP: Flag
IB: HA
Lysate
IB: Flag
IB: GAPDH
F
mock
lipo-ISD
AKT2: WT KO WT KO
IB:pIRF3 (Ser396)
IB:pTBK1 (Ser172)
IB:AKT2
IB:GAPDH
SDS gel
-Dimer
IB:IRF3
-Monomer
Native gel
G
Akt2
IRF3
Hoechst
Merge
IRF3+ nuclei (%)
H
Myc-
HA-AKT2:
Lysate
IP: Myc
IB: HA (short exposure)
IB: HA (long exposure)
IB: Myc
I
14-3-3ζ mRNA (fold)
si14-3-3ζ
Ifnb1 mRNA (fold)
siNC
si14-3-3ζ-1#
IFNβ1 luciferase (fold)
IB: Myc (14-3-3ζ)
IB: GFP
J
Relative 14-3-3ε mRNA level
si14-3-3ε
si14-3-3ε-2#
K
Flag-:
Myc-14-3-3ε:
IP: Flag
IB: HA
IB: Myc
IRF3
IB: Flag
GFP
L
VSV:
HA-AKT2:
Myc-14-3-3ε:
IB:pIRF3 (Ser396)
IB: IRF3
IB: HA
IB: Myc
IB: GAPDH
SDS gel
-Dimer
IB: IRF3
-Monomer
Native gel

Figure EV3.

Figure EV4. The identification of possible phosphorylated sites of IRF3 by AKT2 (related to Fig 4).

A WT or *Akt2* KO PEMs were stimulated with or without VSV for 3 h, then the cell lysates were collected to immunoblot analysis by phosphorylation gel for the assay of phosphorylated IRF3 (the upper band) by anti-IRF3 antibody.

B Mass spectrometry analysis of the frequencies of the phosphorylated sites in IRF3 from HEK293T cells with GFP or AKT2 overexpression.

C, E IFNβ1 luciferase assay (top panels, $n = 3$) of HEK293T-*IRF3* KO cells with overexpression of AKT2 and IRF3 (WT or mutation) for 24 h and challenge with VSV for 6 h. Immunoblot analysis showed the indicated constructs (bottom panels).

D Immunoblot analysis of the p-IRF3 (Ser396) and dimerization of IRF3 in HEK293T-*IRF3* KO cells with the overexpression of the indicated plasmids for 24 h and VSV challenge for 6 h.

F Immunoassay for the translation of the injected mRNAs in the zebrafish embryos.

G Representative images were collected by fluorescence microscope showed GFP-positive (indicating VSV infected) zebrafish larvae where indicated proteins were already expressed for 48 h and challenged with VSV for 18 h. Bars, 300 μm.

Data information: $*P < 0.05$, $**P < 0.01$ and ns, not significant ($P > 0.05$); using a one-way ANOVA test (C and E). Data are from three independent experiments (C and E) or representative of three independent biological replicates (A, D, F). Error bars (C and D, mean ± SEM).
Source data are available online for this figure.

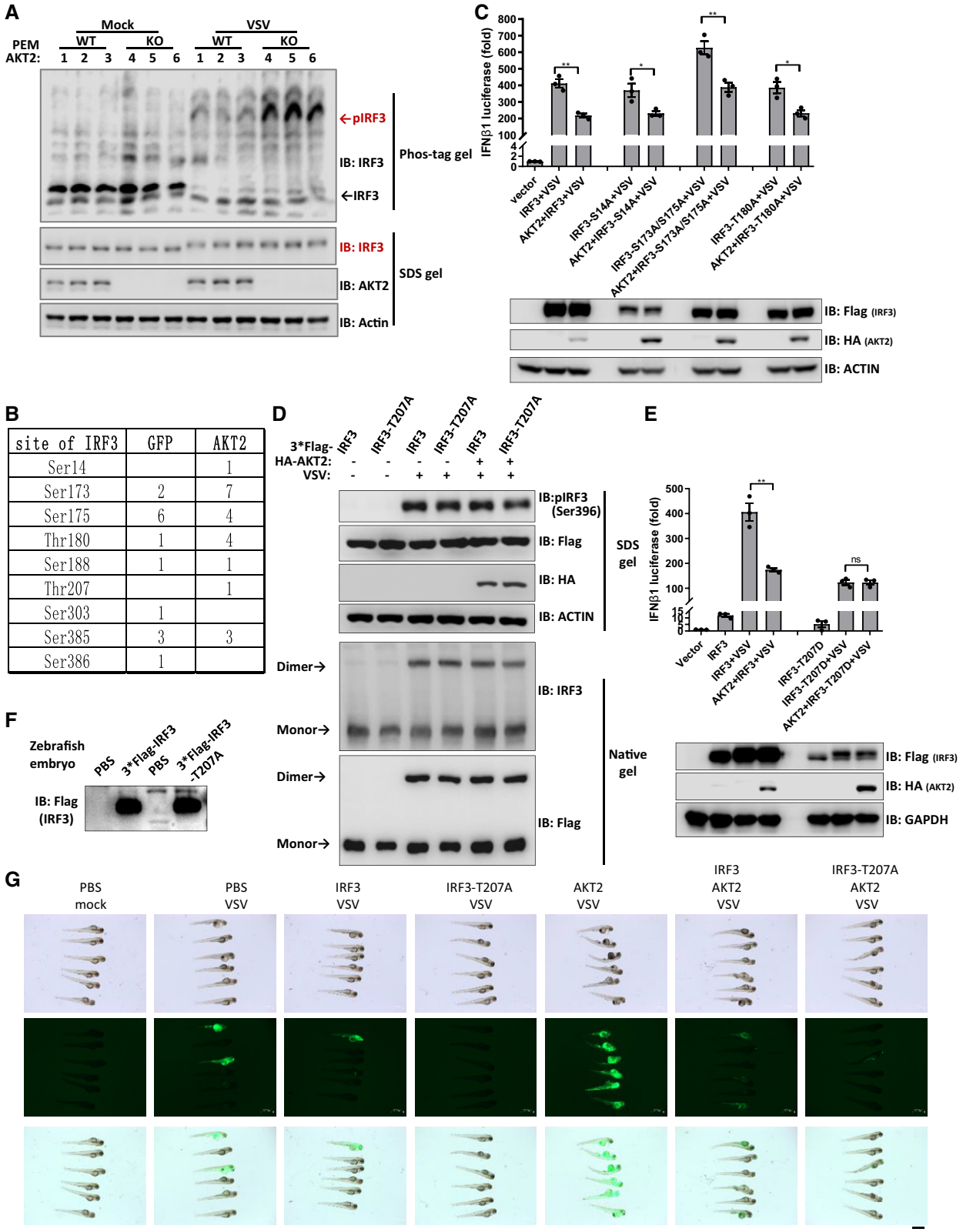
A
Mock
VSV
PEM
WT
KO
AKT2:
1 2 3 4 5 6 1 2 3 4 5 6
←pIRF3
IB: IRF3
←IRF3
Phos-tag gel
IB: IRF3
IB: AKT2
IB: Actin
SDS gel
C
IFNβ1 luciferase (fold)
vector
IRF3+VSV
AKT2+IRF3+VSV
IRF3-S14A+VSV
AKT2+IRF3-S14A+VSV
IRF3-S173A/S175A+VSV
AKT2+IRF3-S173A/S175A+VSV
IRF3-T180A+VSV
AKT2+IRF3-T180A+VSV
IB: Flag (IRF3)
IB: HA (AKT2)
IB: ACTIN
B
site of IRF3 | GFP | AKT2
Ser14 | | 1
Ser173 | 2 | 7
Ser175 | 6 | 4
Thr180 | 1 | 4
Ser188 | 1 | 1
Thr207 | | 1
Ser303 | 1 |
Ser385 | 3 | 3
Ser386 | 1 |
D
3*Flag-
HA-AKT2:
VSV:
IRF3
IRF3-T207A
IB:pIRF3 (Ser396)
IB: Flag
IB: HA
IB: ACTIN
SDS gel
Dimer→
Monor→
IB: IRF3
Native gel
IB: Flag
E
IFNβ1 luciferase (fold)
ns
Vector
IRF3
IRF3+VSV
AKT2+IRF3+VSV
IRF3-T207D
IRF3-T207D+VSV
AKT2+IRF3-T207D+VSV
IB: Flag (IRF3)
IB: HA (AKT2)
IB: GAPDH
F
Zebrafish embryo
PBS
3*Flag-IRF3
3*Flag-IRF3 -T207A
IB: Flag (IRF3)
G
PBS mock
PBS VSV
IRF3 VSV
IRF3-T207A VSV
AKT2 VSV
IRF3 AKT2 VSV
IRF3-T207A AKT2 VSV

Figure EV4.

Figure EV5. The adaptive transfer experiment and the deficiency of Akt2 affect the antiviral response and SLE (related to Figs 5 and 6).

A Schematic diagram of the adoptive transfer experiment (left panel), and FACS analysis of PBMC from reconstructed CD45.1 mice (right panel).

B, C Mice were pretreated with clodronate liposome (200 μl/20 g) before the transfer of WT and *Akt2* KO BMDMs (3 million), and the mice were then challenged with VSV (1×10^6 PFU/g, i.v.) (B). Serum IFNβ1 ($n = 5$) was detected by ELISA 3 h after VSV challenge (C).

D, E qRT–PCR analysis for the relative *Akt2* mRNA expression levels in the PIC ($n \geq 6$), lung ($n \geq 5$) and liver ($n \geq 5$) from TMPD induced murine model of SLE at early stage (2 weeks, A) and late stage (12 weeks, B).

F qRT–PCR analysis of the relative *Akt2* mRNA expression levels in PEMs stimulated with R848 (1 μM) or CpG (1 μg/ml) for 6 h. Mock/R848, $n = 11$; mock/CpG, $n = 17$.

G FACS analysis of the percentages of $CD11b^+$ cells in the spleen of WT and *Akt2* KO mice 2 weeks after TMPD treatment.

H Schematic diagram of the adoptive transfer experiment and TMPD-induced SLE model (upper panel), and FACS analysis of the PBMC from adoptive transferred mice at the indicate time (bottom panel).

I Representative images of lungs (upper panel) and spleens (bottom panel) of WT and *Akt2* KO bone marrow-reconstituted CD45.1 mice treated with TMPD for 12 weeks, and the corresponding images of H&E staining. Bar, 200 μm.

Data information: $*P < 0.05$, $**P < 0.01$, and $***P < 0.001$ and ns, not significant ($P > 0.05$); using unpaired (C–E) or paired (F) *t*-test. Data are pooled from three independent experiments (F) or representative of at least two independent biological replicates (A right panel, C–E, G, H bottom panel, I). Error bars (C–E, mean ± SD). Source data are available online for this figure.

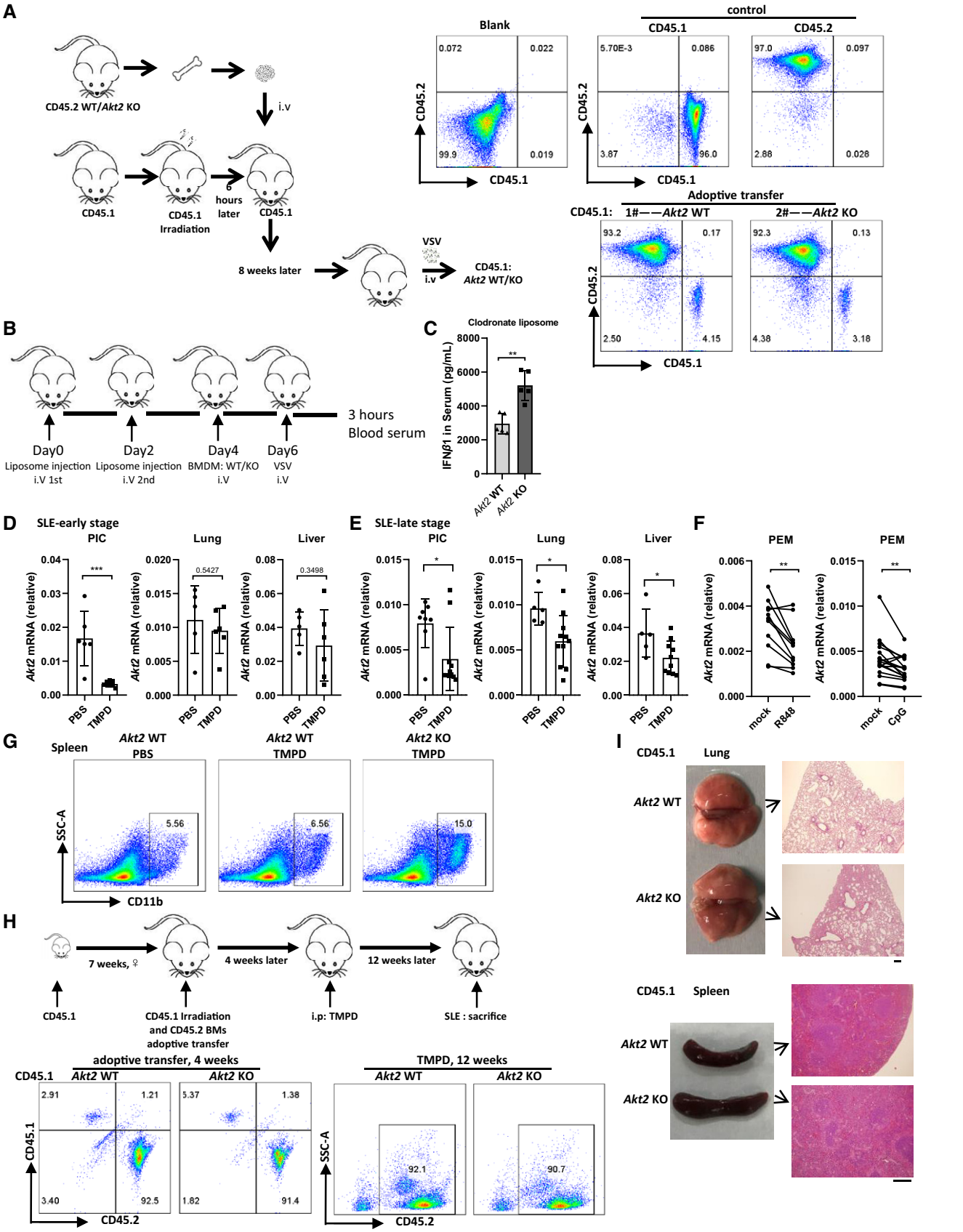
A
CD45.2 WT/Akt2 KO
i.v
CD45.1
CD45.1 Irradiation
6 hours later
CD45.1
8 weeks later
VSV
i.v
CD45.1: Akt2 WT/KO
Blank
control
CD45.1
CD45.2
Adoptive transfer
CD45.1: 1#——Akt2 WT 2#——Akt2 KO
B
Day0 Liposome injection i.V 1st
Day2 Liposome injection i.V 2nd
Day4 BMDM: WT/KO i.V
Day6 VSV i.V
3 hours Blood serum
C
Clodronate liposome
IFNβ1 in Serum (pg/mL)
Akt2 WT
Akt2 KO
D
SLE-early stage
PIC
Lung
Liver
Akt2 mRNA (relative)
PBS
TMPD
E
SLE-late stage
F
PEM
mock
R848
CpG
G
Spleen
Akt2 WT PBS
Akt2 WT TMPD
Akt2 KO TMPD
SSC-A
CD11b
H
7 weeks, ♀
4 weeks later
12 weeks later
CD45.1
CD45.1 Irradiation and CD45.2 BMs adoptive transfer
i.p: TMPD
SLE : sacrifice
adoptive transfer, 4 weeks
TMPD, 12 weeks
I
CD45.1 Lung
Akt2 WT
Akt2 KO
CD45.1 Spleen

Figure EV5.